High performance steel fibre reinforced concrete: residual behaviour at high temperature

Alessio Caverzan · Matteo Colombo · Marco di Prisco · Barbara Rivolta

Received: 17 January 2014 / Accepted: 19 August 2014
Published online: 20 November 2014

A. Caverzan (✉)
Department of Civil and Enviromental Engineering (DICA), Politecnico di Milano, Milan, Italy
e-mail: alessio.caverzan@jrc.ec.europa.eu

Present Address:
A. Caverzan
European Commission Joint Research Centre, IPSC, ELSA, Via E. Fermi, 2749, 21027 Ispra, VA, Italy

M. Colombo · M. di Prisco
Department of Civil and Enviromental Engineering (DICA), Politecnico di Milano, Piazza Leonardo da Vinci, 32, 20133 Milan, Italy

B. Rivolta
Department of Mechanical Engineering, Politecnico di Milano, Via La Masa 1, 20156 Milan, Italy

1 Introduction

High-Performance cementitious composites exhibiting an enhanced elastic limit as well as a strain-hardening response after cracking in bending or even in uniaxial tension have been already developed [10, 24, 26]. The applications of these materials ask the researchers to better investigate the improvement of mechanical characteristics such as fatigue, impact, fire behaviour, durability and shrinkage provided by fibre addition, by adopting the same procedures used in several investigations for plain concrete and for steel fibre reinforced concrete with lower fibre contents [9, 16, 19, 22]. Fire condition is a very important issue in precast concrete structures and the related design is regulated in Europe by European Standard EN 1992-1-2. Researchers are very inter-ested in this matter and some open projects are now investigating fire effects on different kind of struc-tures and in particular on tunnel linings: two large-scale experimental investigations on this matter have being carried out in Austria and in Germany [11, 12]. The use of steel fibre coupled with polypropylene fibre can provide some benefits to structures. First of all, the prevention of spalling phenomena, mainly given by polypropylene fibre, prevents the steel reinforcement (when present) to be directly exposed to fire thus reaching very high temperatures with a consequent mechanical decay and prevents the cross section reduction. Moreover steel fibres give the material a certain residual bending resistance even when exposed to high temperature, improving the bearing capacity of the structure itself [8, 9, 13]. Precast concrete roofing is often disadvantaged by an average dead weight close to 2 kN/m^2, that can be regarded as quite large if compared to the snow load (close to 1.5 kN/m^2). A reasonable compromise in terms of costs and weight can be searched by adopting ultra high performance materials [15], which are more expensive, but can be much lighter. In the technical literature, to the best knowledge of the author, no studies have been reported on the effect of high temperature on the pull-out behaviour of single fibre, but the researchers have focused their attention on the behaviour of the composite as whole [9, 14]. di Prisco et al. [14] studied the mechanical and the thermal properties of a concrete reinforced by steel hooked fibres (30 mm long and with an aspect ratio l_f/d_f equal to 45) at high temperatures. In order to identify the constitutive law in uniaxial tension after a thermal cycle, the authors performed a set of fixed-end tests on double notched prismatic specimen and on notched cylindrical specimen. The results highlight a significant reduction in the peak strength at 400 °C and an expected increase of the ductility for high temperature. In fact, pull-out residual strength is less affected by thermal damage with respect to matrix tensile strength. The results were confirmed by Colombo [7], who studied the thermal and mechanical properties of a fibre reinforced concrete in tension. The author performed several fixed-end tests on cylindrical notched samples in direct tension obtaining similar results. It is worth noting that fibres used by the author were macro fibres and hooked, hence the dominant pull-out mechanism was mechanical [1, 23]. Moreover, these tests do not give any information on the influence of actual temperature (tests in hot condition) on the residual strength, because the tests were carried out at room temperature (20 °C) after cooling. This means that the mechanical characterisation is only significant if the damage introduced by high temperature exposition is related to the maximum temperature reached. An interesting aspect concerns possible differences from the material response at high temperature (hot condition) or after cooling down to room temperature (residual condition); some promising comparison are available in the literature. [19] studied the high-temperature mechanical behaviour of three different materials subjected to direct tension in hot and residual conditions and in compression [18]. The materials investigated were: High-strength concrete (HSC, $f_c = 92$ MPa), a Compact fibre-Reinforced Concrete (CRC, $f_c = 158$ MPa, steel fibres $l_f/d_f = 12/0.4 = 40$ with a content equal to 6 % by volume) and a Reactive-Powder Cementitious mortar (RPC, $f_c = 165$ MPa, steel microfibres $l_f/d_f = 16/0.16 = 100$ with a content equal to 2 % by volume, polymeric fibres with a content equal to 2 % by volume). The authors reported that, up to high temperature ($T = 600$ °C) and after cooling, the direct tensile strengths measured at hot and residual condi-tions were close, particularly for the HSC and PRC but less for CRC. Furthermore, the steel fibres enable CRC to retain up to 50 % of their original strength even after being exposed to 500–600 °C, while HSC and RPC lost 2/3 of their original strength. Considering the fracture energy (which was measured only in the

residual tests), CRC exhibits a strong increase up to 250–300 °C, followed by a steep decrease. In contrast, the lower fracture energy of RPC is hardly affected by the temperature and the extremely reduced fracture energy of HSC (one order of magnitude) is scantly affected by the temperature. These different fracture energy trends point out the role played by steel fibres and suggest a change in the mechanical properties of the fibres and/or the matrix surrounding them with temperature growth. Biolzi et al. [2] investigated the bending behaviour of cementitious material with hybrid fibres exposed to high temperatures and they also performed physical analysis by the use of Mercury Intrusion Porosimetry (MIP) and Scanning Electron Microscope (SEM) observation in order to highlight possible changes in the composites at the microstructure level. Three different fibre cementitious composites (PF: $f_c = 69$ MPa, with polypropylene fibres 0.2 % by volume; SF: $f_c = 116$ MPa, with steel fibres 2 % and SFPF: $f_c = 84$ MPa, with polypropylene fibres 0.2 % and steel fibres 2 % by volume) and one plain cement based composites (NF: $f_c = 96$ MPa) as reference were exposed up to 250, 500 and 750 ° C. The authors observed a signif-icant improvement in the mechanical behaviour of steel fibres composites: an enhancement in strength and strain capacity characterised the test results. In particular, the steel microfibres became weak and brittle and specimens showed a response not influenced by fibres. No fibre pullout was detected in the specimens treated at highest temperature. They observed, by means SEM and Energy Dispersive Spectrometer (EDS) analysis on single steel fibre, that when the maximum temperature reached was equal to 750 ° C, a fibre partial melting occurred and the internal core of fibres was clearly different from the external portion in terms of both morphology and composition. The steel fibres partially melted tended to fill the cracks formed in the concrete. An exchange of material between the external portion of steel fibres and concrete paste took place, as confirmed by the presence of calcium and silica in the fibres. Preliminary results from bending are here presented when the material at room conditions and when a specimen is previously exposed to a maximum temperature of 200, 400 and 600 ° C. On the same material also uniaxial tension tests at low and high strain rates after an exposure to the same maximum temperatures were carried out [3, 4, 5].

2 Material and specimen manufacturing

A mix design HPFRCC proposed by BASF [15] and then optimized by Ferrara et al. [20] was used, the mix design is specified in Table 1. High carbon steel fibres were used with a content equal to 100 kg/m^3 (1.2 % by volume). Polypropylene fibres were not added and spalling phenomena were not observed in tests performed on the HPFRCC material, however this does not exclude spalling occurrence in any condition. The sand used in the material was sieved up to 2 mm and its petrography is listed in Table 2. The petrography analysis was conducted by means of an optical microscope for mineralogy and a stereoscopic microscope. Mineralogic composition and the material structure were analysed and evaluated starting from the constituent optical properties obtained by the optical microscope. The stereoscopic microscope was used to define morphological characteristics as sphericity, color or materials which could alterate the surface. The sand used can be defined as quartz sand mixed. To similar

Table 1 Mix design

Constituent	Dosage (kg/m^3)
Cement type I 52.5	600
Slag	500
Water	200
Super plasticizer	33 l/m^3
Sand 0–2 mm	983
Fibres ($l_f = 13$ mm; $d_f = 0.16$ mm)	100

Table 2 Sand petrography

Constituent	%
Quartz	47.7
	(35.9 monocrystalline)
	(11.8 polycrystalline)
Gneiss	15.5
Feldspar	9.5
Micas and mica schist	6.4
Granitoids rocks	5.1
Microcrystalline silica	2.7
Amphibolis	2.7
Carbonate rocks	2.4
Siltstone	2.4
Serpentinites	1.4
Garnet and iron oxides	0.7

results in terms of mix Ferrara et al. [20] arrived following a methodology for mix optimization done step by step starting from cement paste and moving towards high performance fibre reinforced cementitious com-posites by adding growing fibre contents. The cylindrical compressive strength was close to 110 MPa. Fibres were straight, 13 mm long and with an aspect ratio (l_f/d_f) equal to 80. Specimens were all extracted from a slab 1.6 m × 0.64 m in plane, 30 mm thick. The slab was cast by applying a unidirectional flow as shown in Fig. 1. In order to guarantee a certain fibre orientation the proprieties of the self compacting material were used taking advantage of the flow direction. Three prismatic beam samples, 40 mm wide, 30 mm thick and 600 mm long, were sawed from the slab and tested at room temperature to perform a proper mechanical characterization of the material according to Italian Guidelines [6]. The high fibre content and the favourable orientation imposed by the casting flow control allowed us to guarantee a small dispersion of the response before and after single-crack localization and a hardening behaviour in uniaxial tension [4]. Nine beam specimens, with the same geometry, were used to investigate the thermal decay of multi-localization and single-localization cracking phases and the change of residual strengths in bending after exposure to high temperatures. The samples reported in Fig. 1 without reference will be used for future experimental campaign in hot conditions.

3 Experimental programme

3.1 Thermal treatment

The thermal treatment of the samples was carried out in an electric furnace by performing thermal cycles up

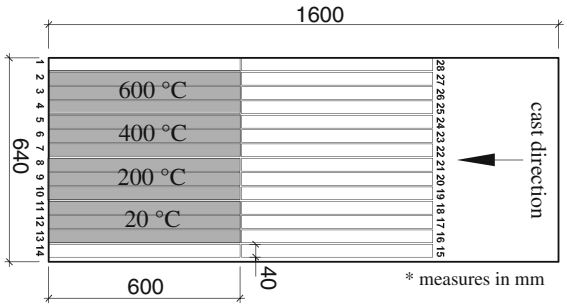

Fig. 1 Slab cast applying a unidirectional flow

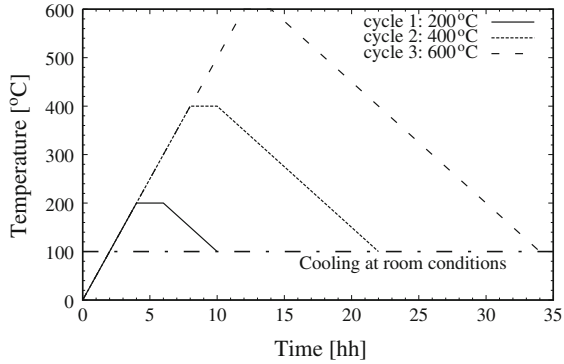

Fig. 2 Thermal cycle imposed

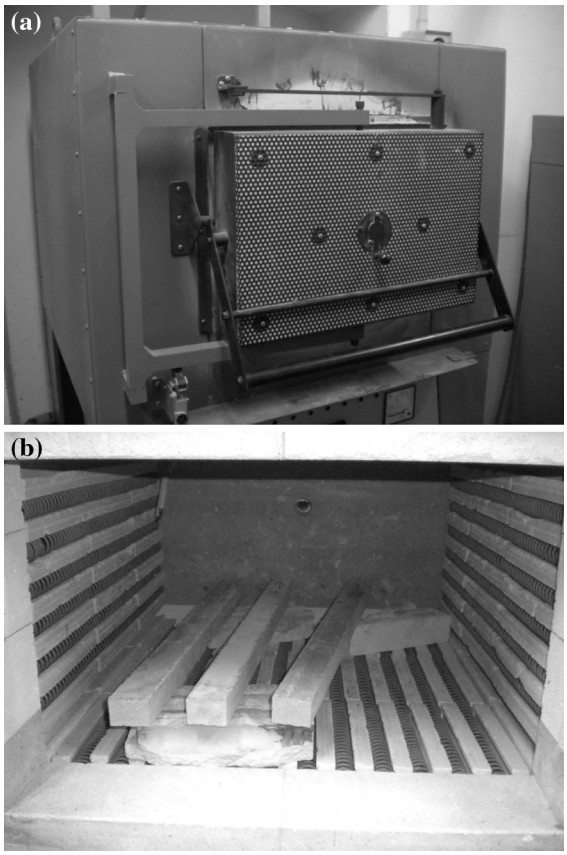

Fig. 3 Device used to perform the thermal treatment

to different maximum temperatures. Three maximum temperatures thresholds (200, 400 and 600 °C) were reached. A heating rate equal to 50 °C/h was imposed up to the maximum thresholds, and after two hours of stabilization ensured a homogeneous temperature

distribution within the sample volume. The temperature was after reduced with a rate of 25 °C/h down to 100 °C and then a cooling process at room temperature was carried out (Fig. 2). The temperature was measured by means of a thermocouple placed inside the furnace. Felicetti and Ferrara [17] established, using the same furnace and material, that the thermal cycle adopted guarantee a maximum difference in terms of temperature between furnace and samples equal to about 1–2 °C. For each cycle, three nominally identical samples (Fig. 3) were introduced into the furnace.

3.2 Third point bending tests

Third point bending tests were performed to study the mechanical properties of the material after the heat treatment described previously. More precisely, tests were performed 2 weeks after the end of the cooling process. The loading scheme (Fig. 4) refers to a span between the supports of 450 mm and a spacing between the loading knives of 150 mm. It is worth highlighting that the samples were unnotched, and thus a multi-crack pattern could be found before the single-crack localisation during the bending tests, as discussed later on. Stroke was considered as feedback parameter during the tests. The displacement rate was imposed equal to 1.87×10^{-2} mm/s in each test. Two LVDT transducers (long. bottom 1, 2 in Fig. 4) were used to measure the relative displacements with a gauge length equal to 200 mm. This measure, in the following named crack opening displacement (COD), considers two different deformation terms: the elastic strain that characterises the pre-cracking test phase, and the crack opening width corresponding to multi- or single-crack occurrence, respectively, in the hardening (where for example 25–30 visible cracks were counted in the thermal undamaged samples) or softening regions corresponding to the pre- and post-peak regions. For each temperature (200, 400 and 600 ° C) three samples were tested. In order to compare the mechanical properties at high tempera-ture with those of the undamaged material, three prismatic specimens with the same geometry and with the same set-up were tested at room temperature.

3.3 Tensile tests on wire samples

In order to investigate mechanical properties of the fibre at room condition and their decay after a thermal treatment, several steel wires were tested in uniaxial tension. Two meter long steel wire samples were cut from a skein (Fig. 5a) used to produce the fibres. A thermal treatment, identical to the one used for un-notched prismatic samples (Sect. 3.1), was applied to one of the wire sample. Uniaxial tension tests were carried out on 2 m long wires with a 0.16 mm nominal diameter, fixed to the testing machine by means of a couple of reels. Both the wire ends were wound to the reel for a length equal to 850 mm in order to assure a good frictional support during the tests, the span between the reels was equal to 300 mm. Stroke was considered as feedback parameter during the tests. The displacement rate imposed during the tests was equal to 1×10^{-3} mm/s. The results of tensile tests are

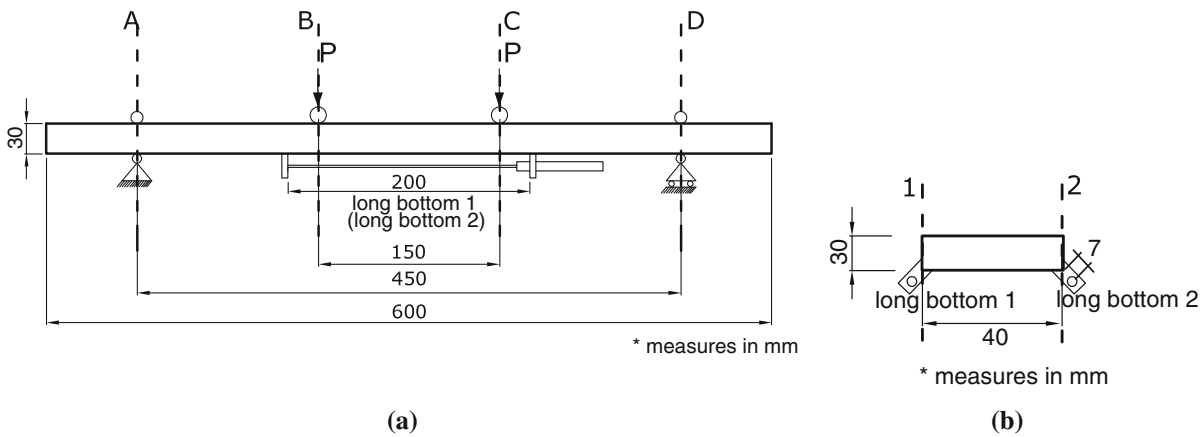

Fig. 4 Un-notched beam specimen load scheme: **a** longidutinal view; **b** cross section

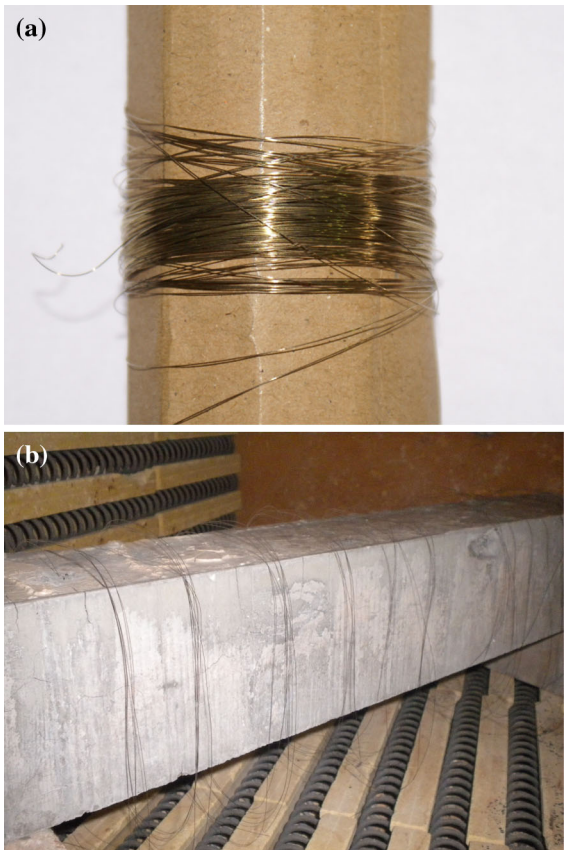

Fig. 5 Skein used to produce the fibres (**a**) and the wires samples in the furnace (**b**)

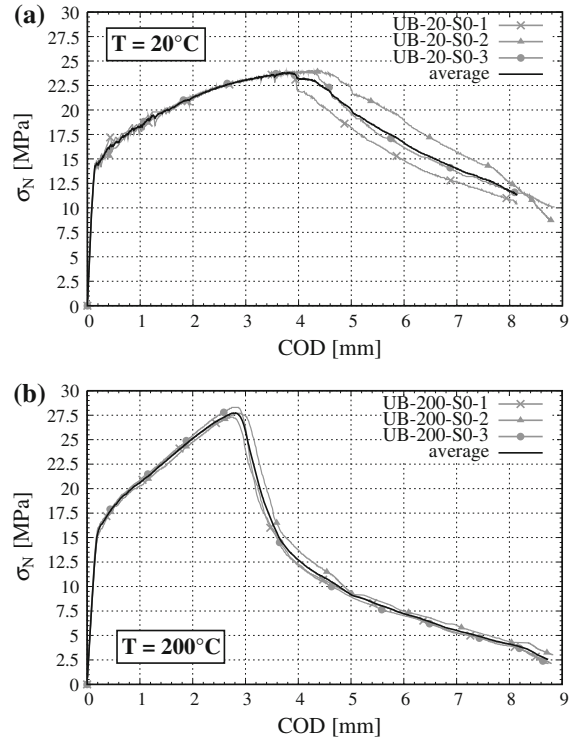

Fig. 6 Stress versus COD curves. Tests carried out on: **a** undamaged specimens (UB-20-S0); **b** specimens exposed up to 200 °C (UB-200-S0)

listed in Table 5 for temperature of 20 and 600 °C in terms of nominal stress ($\sigma_N = \frac{P}{A}$ where P is the load and A the wire cross section) versus stroke displacement, respectively.

4 Tests results

4.1 Bending tests

Results of third point bending tests are shown in Figs. 6 and 7 in terms of nominal stress (σ_N) versus crack opening displacement (COD of multi-crack stage), where nominal stress is defined as follows:

$$\sigma_N = \frac{6M}{bh^2} \tag{1}$$

with M is the bending moment acting between the loading knives; b is the width of the specimen; h the thickness of the specimen.

The mechanical strength of the tested specimens are listed in Tables 3 and 4. The results are shown in Figs. 6a, b and 7a, b for temperatures 20, 200, 400 and 600 ° C, respectively; the comparison among the average curves is shown in Fig. 8. The meaning of each parameter listed in Table 4 is explained as follows:

- f_{If}: first cracking strength, representing the matrix flexural tensile strength, is the maximum strength in the COD range 0–0.1 mm. Due to the hardening behaviour in bending after first cracking, the maximum value, in the investigated range, is always considered, and it is refereed to as w_{I};
- w_{I}: conventional COD when the first crack is assumed to propagate;
- f_{eq1}: average nominal strength in COD range between $3w_{\mathrm{I}}$ and $5w_{\mathrm{I}}$ (0.3–0.5 mm) that is considered as a reference for Serviceability Limit State (SLS) residual strength;
- f_{eq2}: average nominal strength in COD range between $0.8w_{\mathrm{u}}$ and $1.2w_{\mathrm{u}}$, which is regarded as

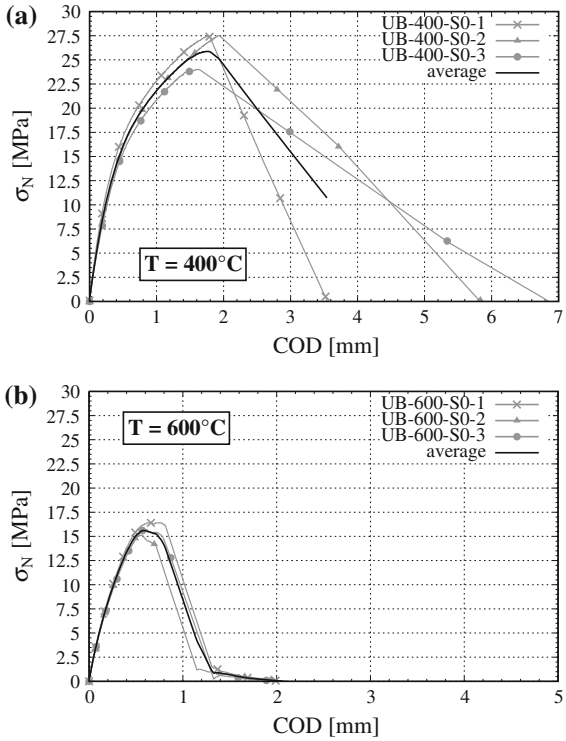

Fig. 7 Stress versus COD curves. Tests carried out on: **a** specimens exposed up to 400 °C (UB-400-S0); **b** specimens exposed up to 600 °C (UB-600-S0)

Ultimate Limit State (ULS), when material behaviour is governed only by pull-out mechanism.

w_u is the ultimate COD. In the Italian Guidelines [6] it is defined, for bending, as the minimum crack opening between 0.02 l_{cs} and 3 mm, where l_{cs} is the structural characteristic length assumed equal to the specimen cross section depth. In the present research work, it was chosen to follow a different definition to compute the ultimate crack opening value, by correctly taking into account the multilocalisation process, as suggested by Ferrara et al. [21]. This allows to prevent any superposition with the serviceability COD ranges already considered. A very small dispersion of the mechanical response for each group of tests can be observed in the experimental curves. Low values of standard deviation coefficients (see Table 4, with particular reference to f_{lf} and f_{eq1}, indicate a good fibre orientation and a homogeneous dispersion in the matrix. The casting procedure used to prepare the slab was chosen to favour a profitable fibre orientation, and thus achieved the maximum benefits from fibre addition. It is also very interesting to highlight that the mechanical behaviour derived from the tests at room temperature (Fig. 6a) are hardening in bending with a first pre-peak multi-localisation phenomenon followed by a single crack localisation in the post peak region as highlighted in Fig. 9; a peak tensile strain equal to 2 %, measured at the bottom fibre of the cross section, was reached (Table 3). Tests performed after an exposure to a maximum temperature of 400 °C could be regarded as hardening in bending up to more than 2.8 mm of the relative displacement measured at the bottom fibre. Nonetheless, although the value is quite high, it is not high enough to define the material as hardening in bending according to the established

Table 3 Strengths and COD at the peak load and ultimate COD

Sample code	COD_{peak} (mm)	$COD_{peak,av}$ (mm) (SD)	f_{peak} (MPa)	$f_{peak,av}$ (MPa) (SD)	w_u^* (mm)	$w_{u,av}^*$ (mm) (SD)
UB-20-1	3.78	4.17 (0.35)	23.90	23.93 (0.06)	3.81	3.94 (0.11)
UB-20-2	4.44		24.00		4.00	
UB-20-3	4.30		23.90		4.00	
UB-200-1	2.77	2.85 (0.07)	27.30	27.77 (0.99)	2.95	3.02 (0.06)
UB-200-2	2.91		27.70		3.07	
UB-200-3	2.87		28.30		3.04	
UB-400-1	1.80	1.79 (0.15)	27.40	26.30 (1.99)	2.13	2.12 (0.13)
UB-400-2	1.94		27.50		2.24	
UB-400-3	1.64		24.00		1.99	
UB-600-1	0.77	0.65 (0.11)	16.40	15.73 (0.65)	1.28	1.17 (0.10)
UB-600-2	0.57		15.10		1.10	
UB-600-3	0.62		15.70		1.12	

Table 4 First cracking and residual strengths (specimens UB)

Sample code	f_{lf} (MPa)	$f_{lf,av}$ (MPa) (SD)	f_{eq1} (MPa)	$f_{eq1,av}$ (MPa) (SD)	f_{eq2} (MPa)	$f_{eq2,av}$ (MPa) (SD)
UB-20-1	11.50	11.30 (0.35)	16.41	15.98 (0.46)	22.54	23.14 (0.56)
UB-20-2	11.50		15.50		23.64	
UB-20-3	10.90		16.02		23.25	
UB-200-1	9.51	9.10 (0.36)	17.46	17.37 (0.32)	23.29	23.42 (0.47)
UB-200-2	8.91		17.12		23.94	
UB-200-3	8.88		17.53		23.02	
UB-400-1	5.54	4.93 (0.53)	15.03	13.97 (0.93)	21.92	23.23 (1.92)
UB-400-2	4.65		13.53		25.44	
UB-400-3	4.59		13.35		12.42	
UB-600-1	4.78	4.64 (0.19)	13.61	13.16 (0.47)	3.64	4.36 (1.96)
UB-600-2	4.72		13.20		3.51	
UB-600-3	4.42		12.67		5.92	

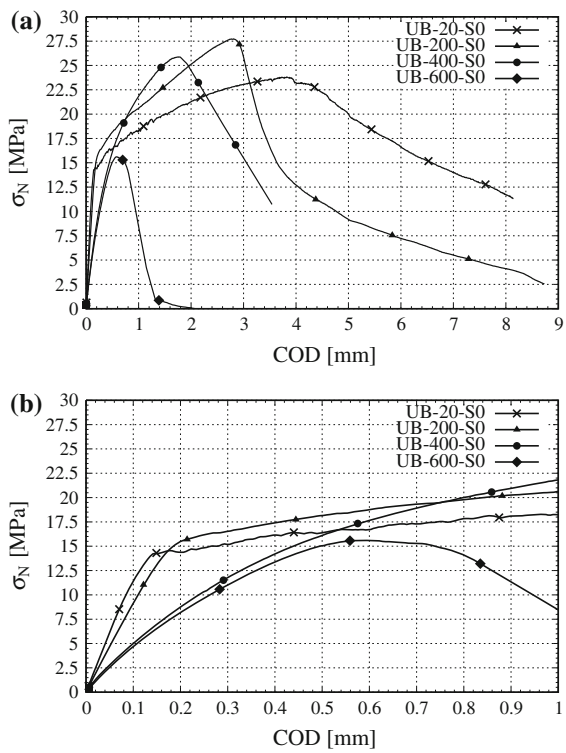

Fig. 8 Stress versus COD average curves. Tests carried out on UB specimen: **a** average curves; **b** detail of the peak zone

international requirements [25] that impose a bending strain of 2 %. Considering that the loading knife spacing is equal to 150 mm, and assuming a perfect spreading on such zone, it would result in a COD of 3 mm. It is interesting to observe that these results cannot be achieved by testing notched specimens. This

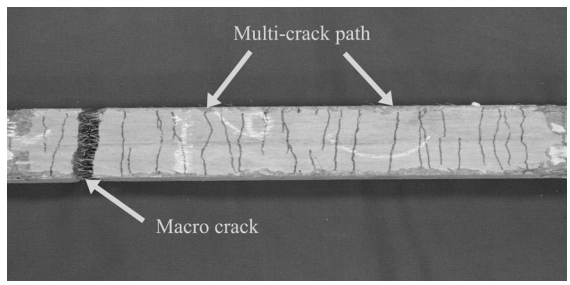

Fig. 9 Multi- and single-crack pattern

because the notch induces crack localisation only in the middle cross section and, moreover, it reduces the matrix strength causing the increase in the stress intensity factor. On the other hand, neither three point bending testing is appropriate, since it cannot take into account the topological variability of the material in a large span length, due to fibre dispersion. Only direct tension testing on unnotched specimens can assure a hardening tensile response as that derived. Different values of w_u^* should be used instead of the COD values suggested by the Italian Guidelines to investigate the effective ductility of the hardening branch. The reference values could be computed as follows:

$$w_u^* = \begin{cases} (0.02 - \varepsilon_{peak})h + \varepsilon_{peak} L_{COD} & \text{if } \varepsilon_{peak} < 0.02 \\ 0.02 L_{COD} & \text{if } \varepsilon_{peak} \geq 0.02 \end{cases} \quad (2)$$

where L_{COD} represents the gauge length used to measure COD displacement and ε_{peak} is the peak strain computed according to the following equation:

$$\varepsilon_{peak} = \frac{COD_{peak}}{L_{COD}} \quad (3)$$

It has to be noted that the gauge length is assumed 50 mm longer than that of the load span. In fact, though in the zone adjacent to the loading knives the bending moment, computed according to the beam theory, is lower than that between the loading knives, localised stresses can arise. These possibly lead to the generation and propagation of cracks outside the loading span. The values computed according to Eq. 2 are reported in Table 3.

Moving to the analysis of the test results related to the specimens exposed to high temperatures (200, 400 and 600 °C), the first-crack strength (Table 4) and the stiffness are the parameters more relevantly affected by the prior thermal damage. Tests on material exposed to 400 °C show a large multi crack phase up to 0.9 mm of COD (Table 3) followed by a softening branch, related to a macro crack opening. Although the initial stiffness decreases with the increasing temperature, and the value of f_{eq1} is comparable with the strengths computed for the samples treated at 400 °C, the pre-peak ductility is reduced at 600 °C, and the post-cracking branch becomes very steep, thus limiting the overall toughness of the material. Thermal treatment up to 600 °C seriously reduces the mechanical properties of the steel fibres, as shown by Figs. 11 and 12. The fracture surfaces exhibit a large number of failed fibres (Fig. 11a) with respect to the pulled out ones (Fig. 11b), as already reported by Biolzi et al. [2]. Furthermore, an oxidised film covers the lateral fibre surface (Fig. 12a, b), which can affect bond at the interface between the fibre and the matrix. The type of fibre failure shows a significant ductility up to 400 °C and the ratio between f_{eq2} and f_{eq1} confirms the hardening in bending definition ($f_{eq2}/f_{eq1} = 1.66$). When residual tests at 600 °C are considered, the post-peak behaviour

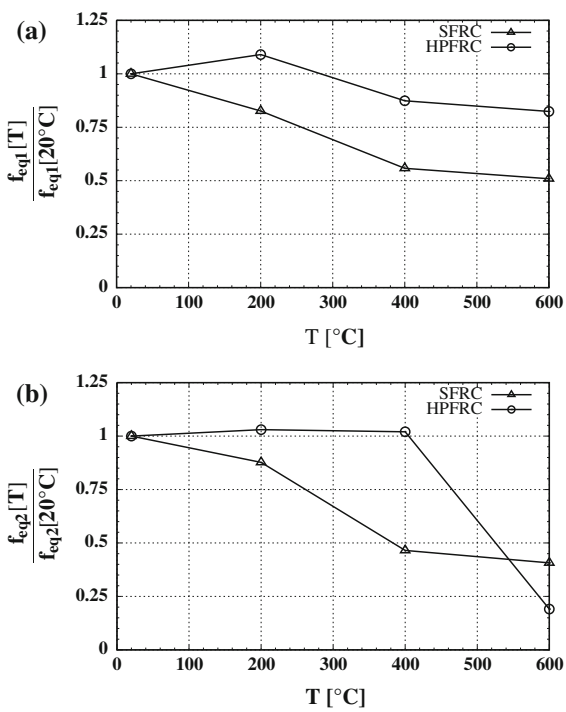

Fig. 10 Residual strengths versus temperature for SFRC ($R_c = 75$ MPa, $V_f = 0.66$; $l_f/d_f = 80$, $l_f = 30$ mm [7]) and HPFRC materials: $f_{eq1}(T)/f_{eq1}$ (20 °C versus temperature (**a**); $f_{eq2}(T)/f_{eq2}$ (20 °C) versus temperature (**b**)

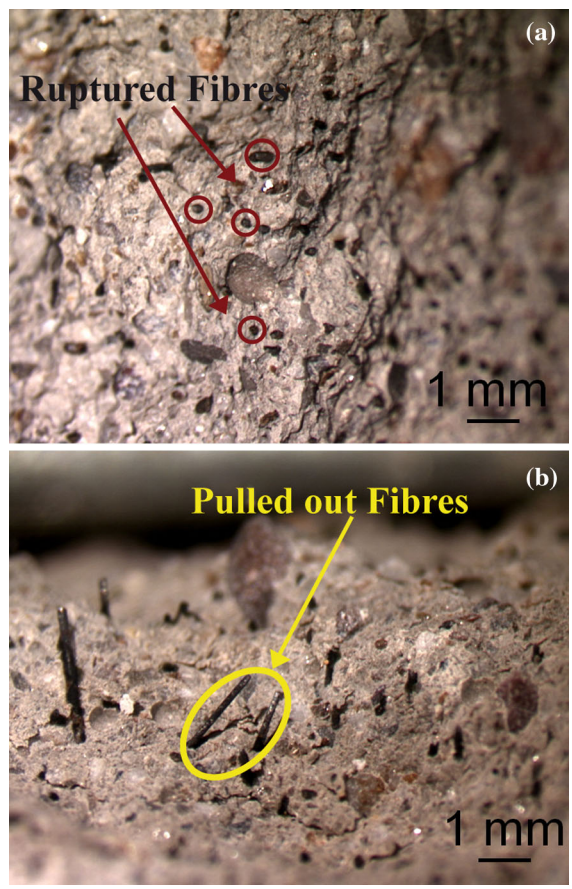

Fig. 11 Fracture surface on specimens previously exposed to a thermal cycle up to 600 °C: fibres failed (**a**); fibres pulled-out (**b**)

becomes softening and quite brittle ($f_{eq2}/f_{eq1} = 0.33$): a high toughness at the macro-scale, guaranteed by pull out mechanism, requires at the fibre level a significant slip between fibre and matrix without any failure. When the material is exposed to 600 °C, the fibre failure is confirmed by the pictures taken on the macro-crack surface (Figs. 11, 12). Finally, on the basis of the equivalent strengths, defined by taking into account the pre-peak ductility, it is possible to show that the residual equivalent strengths change with the increase in temperature (Fig. 10) differently from steel fibre reinforced concrete characterised by a low content of fibres (<0.7 %). The comparison clearly highlights the surprising performances of such materials in terms of its fire resistance behaviour.

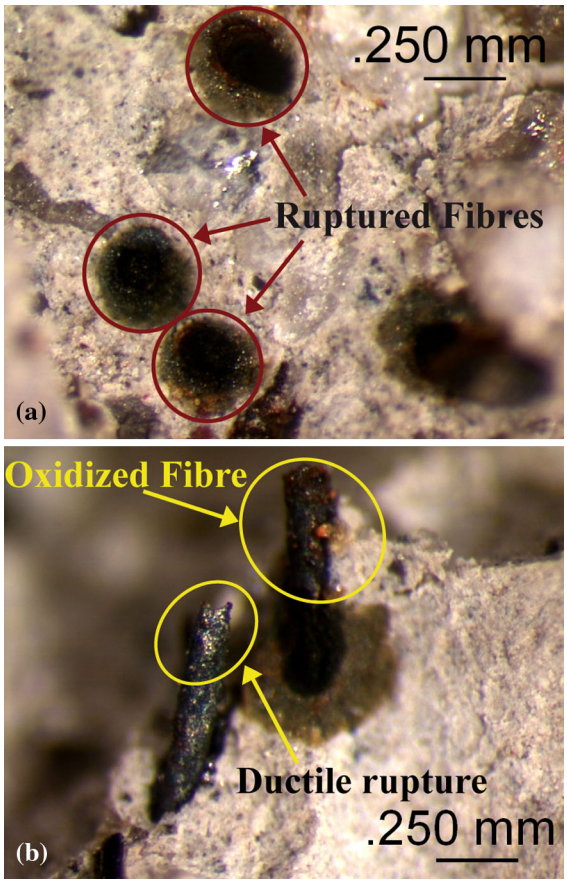

Fig. 12 Fracture surface on specimens previously exposed to a thermal cycle up to 600 °C: detail of fibres failed (**a**); fibres oxidized (**b**)

4.2 Tensile tests on wire

As mentioned in the previous paragraph, in order to evaluate the influence of high temperatures on the fibre mechanical properties, a series of tensile tests on High strength steel wire specimens at room conditions were carried out. Six wires undamaged samples were tested and considered as reference samples. Six wires were subjected to a thermal treatment performed in an electrical furnace up to 600 °C applying the same heating and cooling rates adopted for the unnotched beam specimens and previously described (Fig. 2). A fibre inside a beam sample should be subjected to different types of thermal cycles depending on its position with respect to the boundary surface. The thermal cycle imposed is the closest to the real thermal conditions to a fibre close to the boundary surface (i.e. a surface subject to a tensile stress during a bending test) applied during the unnotched beam thermal treatment. However, Felicetti and Ferrara [17] established, using the same furnace and material, that the thermal cycle adopted with a two hour of

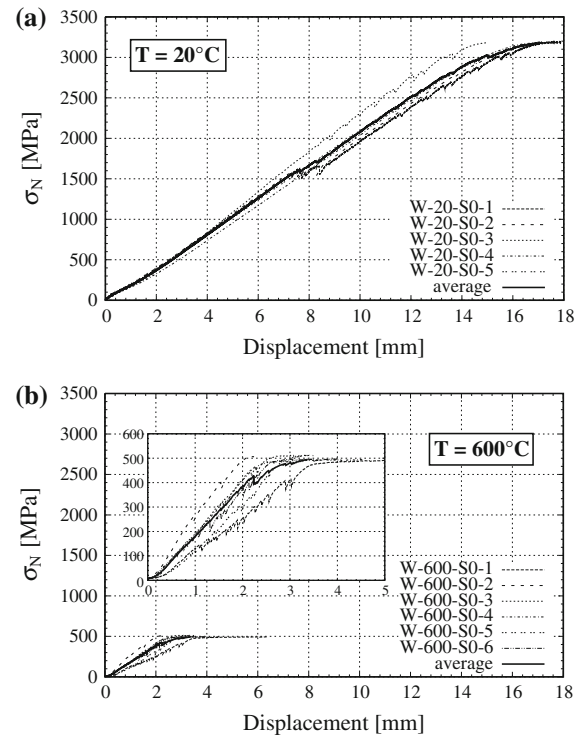

Fig. 13 Stress versus displacement curves. Tests carried out on: undamage specimens W-20-S0 (**a**); specimens exposed up to 600 °C W-600-S0 (**b**)

stabilization phase ensures an homogeneous temperature in all the HPFRCC samples and in the fibres, hence the thermal damage imposed to wires tested can be considered equal to the one affected by fibres in a unnotched beam sample. Specimens exposed up to 600 °C show an abrupt tensile strength decay passing from 3,180 MPa of the undamaged wire to 500 MPa (Table 5; Fig. 13a, b). In order to enlighten the change in the wire microstructure, a microscope analysis was carried out after polishing and Nital 1 %etching. Both transversal and longitudinal cross sections were investigated before and after the thermal treatment exploiting an optical microscope. Figures 14 and 16a show as the undamaged fibres are characterised by ferritic-pearlitic high deformed microstructure. The pearlitic grains, which were spheroidal in origin, are stretched during the drawing process (dark areas in Fig. 16a). After the thermal treatment up to 600 °C, the micro structure changes and a ferritic-pearlitic structure with a globular shape carbides can be recognised (dark areas in Figs. 15, 16b). Moreover, an oxide film 20 μm thick, covering the external wire surface, was observed (Fig. 15a, b). The measure of the wire diameter, before and after the

Table 5 Peak strength and displacement (specimens W)

Sample code	σ_{peak} (MPa)	δ_{peak} (mm)
W-20-S0-1	3,187	17.67
W-20-S0-2	3,190	17.21
W-20-S0-3	3,181	14.99
W-20-S0-4	3,178	16.92
W-20-S0-5	3,183	17.25
W-600-S0-1	494	6.31
W-600-S0-2	507	2.21
W-600-S0-3	512	2.91
W-600-S0-4	495	4.49
W-600-S0-5	513	3.42
W-600-S0-6	562	2.63
W-600-S0-7	497	3.02

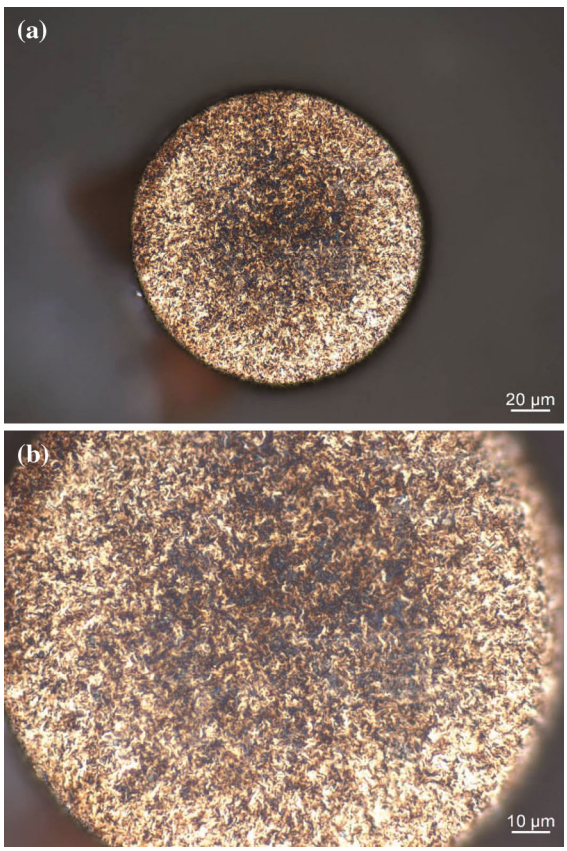

Fig. 14 Details of the undamage wire cross section

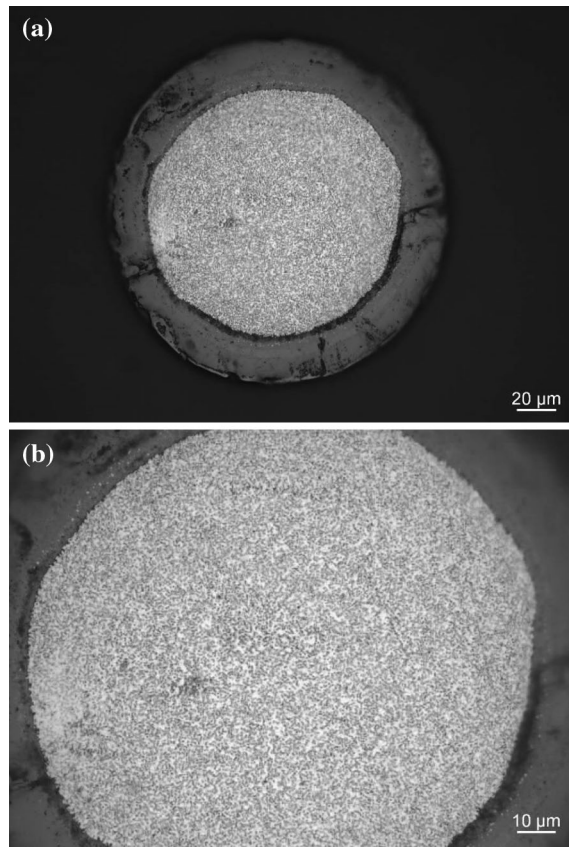

Fig. 15 Details of the wire cross section after exposure up to 600 °C

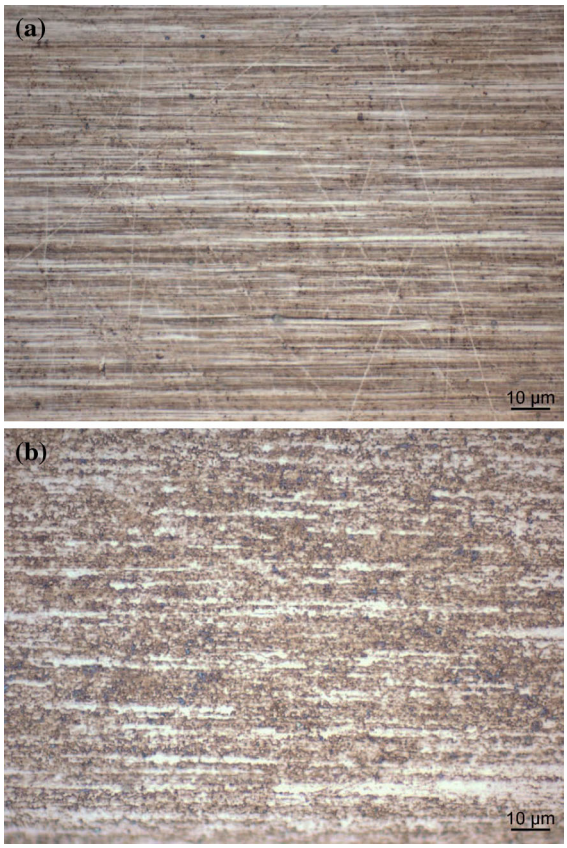

Fig. 16 Details of the wire longitudinal section: undamage specimens (**a**); specimens exposed up to 600 °C (**b**)

thermal treatment, detected an increase of about 0.02 mm, this being partly due to the developed oxide film. This increase in the sectional area, coupled with the decay in the tensile strength due to microstructural change, compromises the effectiveness of the pull-out mechanism and explains the material embrittlement when exposed to high temperatures (Tables 3 and 4).

5 Conclusions

The experimental investigation on high tempera-ture behaviour of high performance steel fibre reinforced cementitious composite used for light precast roof elements suggests the following con-cluding remarks:

– By suitably orienting the casting flow of the self compacting composite, it is possible to significantly reduce the scattering and produce very efficient materials in terms of mechanical performances in uniaxial tension with a fibre content of about 1.2 % of high carbon steel fibres.
– The material so cast, and thus characterised by a good fibre alignment, showed a very high performance compared with other cementitious composites at comparable costs.
– The material shows an impressive response at high temperatures in bending; it remains hardening in bending up to a thermal exposure of 400 °C. The serviceability and the ultimate strengths are scantly affected by the thermal damage. Only the initial stiffness and the peak deformation decrease. The high performances showed in bending were confirmed also in the tensile static tests. At room conditions the material exhibited a parabola-rectangular behaviour with a significant stress plateau which becomes weakly softening at 200 °C.
– For an exposure of 600 °C the material becomes softening in bending and a decay of about 65 % is produced on ultimate residual strengths, even if a peak strength of more than 60 % equivalent to 15 MPa are still available.
– The material exposed to 600 °C fails due to steel fibre rupture, this behaviour being prevailingly due to the damage caused to the fibres by the high temperature. Thermal treatment up to 600 °C was shown. The significant decay of the fibres mechanical properties can be ascribed to the change in the fibre microstructure and an evident reduction of the cross section. Moreover, fibres exposed to 600 °C appear covered by an oxide film, which could affect the bond between the fibres and the matrix.

Acknowledgments The research was partially financed by the project ACCIDENT ID 501 7629770 in the frame of INTERREG IT/CH 2006–2013 program.

References

1. Alwan JM, Naaman AE, Guerrero P (1999) Effect of mechanical clamping on the pull-out response of hooked steel fibers embedded in cementitious matrices. Concr Sci Eng 1(1):15–25
2. Biolzi L, Guerrini G, Bertolini L (2004) Cementitious materials with hybrid fibers exposed to high temperatures. In: di Prisco M, Felicetti R, Plizzari GA (eds) 6th

Symposium on fibre reinforced concrete (FRC), BEFIB2004, RILEM Proceedings. RILEM, Varenna, Italy, pp 635–646
3. Caverzan A, Cadoni E, di Prisco M (2012) Dynamic behavior of HPFRCC at high strain rate: the fiber role. In: High performance fiber reinforced cement composites 6. Springer, Netherlands, pp 339–346
4. Caverzan A, Cadoni E, di Prisco M (2012) Tensile behaviour of high performance fibre-reinforced cementitious composites at high strain rates. Int J Impact Eng 45:28–38
5. Caverzan A, Cadoni E, di Prisco M (2013) Dynamic tensile behaviour of high performance fibre reinforced cementitious composites after high temperature exposure. Mech Mater 59:87–109
6. CNR-DT 204 (2006) Guidelines for the design, construction and production control of fibre reinforced concrete structures. National Research Council of Italy
7. Colombo M (2007) FRC bending behaviour: a damage model for high temperatures. PhD thesis, Politecnico di Milano
8. Colombo M, di Prisco M (2003) SFRC: a damage model to investigate the high temperature mechanical behaviour. In: Bicanic N, de Borst R, Mang H, Meschke G (eds) Computational modelling of concrete structures EURO-C 2003, Rotterdam, pp 309–318
9. Colombo M, di Prisco M, Felicetti R (2010) Mechanical properties of steel fibre reinforced concrete exposed at high temperatures. Mater Struct 43:475–491. doi:10.1617/s11527-009-9504-0
10. Dawood ET, Ramli M (2011) High strength characteristics of cement mortar reinforced with hybrid fibres. Constr Build Mater 25(5):2240–2247
11. Dehn F, Werther N (2006) Burning tests at the tunnel inner concrete shell for the m 30 north tunnel in madrid [brandversuche an tunnelinnenschalenbetonen für den m 30-nordtunnel in madrid]. Beton- und Stahlbetonbau 101(9):729–731 [cited by (since 1996) 2]
12. Dehn F, Nause P, Fischkandl H (2008) Fire-resistant concrete for tunnel construction [brandresistenter beton für den tunnelbau]. Beton- und Stahlbetonbau 103(4):271–277 [cited By (since 1996) 1]
13. di Prisco M, Felicetti R, Colombo M (2003a) Fire resistance of sfrc thin plates. In: Bicanic N, de Borst R, Mang H, Meschke G (eds) Computational modelling of concrete structures. EURO-C 2003, Rotterdam, pp 783–792
14. di Prisco M, Felicetti R, Gambarova P (2003b) On the fire behavior of sfrc and sfrc structures in tension and bending. In: Reinhardt HW, Naaman AE (eds) High performance fiber reinforced cement composites (HPFRCC-4), RILEM Proceedings. RILEM, Bagneux, pp 205–222
15. di Prisco M, Lamperti M, Lapolla S, Khurana R (2008) Hpfrcc thin plates for precast roofing. In: Fehling E, Schmidt M, Sturwald S (eds) Ultra high performance concrete: proceedings of the 2nd international symposium on ultra-high performance concrete, No. 10 in Structural materials and engineering series. Kassel University Press, Kassel, pp 675–682
16. di Prisco M, Plizzari G, Vandewalle L (2009) Fibre reinforced concrete: new design perspectives. Mater Struct 42:1261–1281. doi:10.1617/s11527-009-9529-4
17. Felicetti R, Ferrara L (2008) The effect of steel fibre on concrete conductivity and its connection to on-site material assessment. In: Gettu R (ed) 7th Symposium on fiber reinforced concrete (FRC), BEFIB2008. RILEM, Chennai, pp 525–536
18. Felicetti R, Gambarova PG (1998) Effects of high temperature on the residual compressive strength of high-strength siliceous concretes. ACT Mater J 95(4):395–406
19. Felicetti R, Gambarova P, Natali Sora M, Khoury G (2000) Mechanical behaviour of hpc and uhpc in direct tension at high temperature and after cooling. In: Rossi P, Chanvillard G (eds) 5th Symposium on fibre reinforced concrete (FRC), BEFIB2000, RILEM Proceedings. RILEM, Lyon, pp 749–758
20. Ferrara L, Park YD, Shah SP (2008) Correlation among fresh state behavior, fiber dispersion, and toughness properties of sfrcs. J Mater Civ Eng 20(7):493–501. http://link.aip.org/link/?QMT/20/493/1
21. Ferrara L, Ozyurt N, di Prisco M (2011) High mechanical performance of fibre reinforced cementitious composites: the role of "casting-flow induced" fibre orientation. Mater Struct 44:109–128. doi:10.1617/s11527-010-9613-9
22. Ferrara L, Bamonte P, Caverzan A, Musa A, Sanal I (2012) A comprehensive methodology to test the performance of steel fibre reinforced self-compacting concrete (SFR-SCC). Constr Build Mater 37:406–424
23. Kim D, El-Tawil S, Naaman A (2008) Loading rate effect on pullout behavior of deformed steel fibers. ACI Mater J 105(6):576–584
24. Mechtcherine V (2007) Testing behavior of strain hardening cement-based composites in tension—summary of recent research. In: Reinhardt HW, Naaman AE (eds) High per-formance fiber reinforced cement composites (HPFRCC-5), RILEM Proceedings, vol 53. RILEM, Mainz, pp 13–22
25. Model Code (2010) CEB-FIP Model Code 2010. Comité Euro-International du Béton, Lausanne
26. Naaman A, Reinhardt H (2006) Proposed classification of hpfrc composites based on their tensile response. Mater Struct 39(5):547–555